Bioorganic Chemistry 83 (2019) 336–347

Contents lists available at ScienceDirect

Bioorganic Chemistry

journal homepage: www.elsevier.com/locate/bioorg

Design, synthesis and bioevaluation of tricyclic fused ring system as dual binding site acetylcholinesterase inhibitors

Saba Tahir Tanoli[a], Muhammad Ramzan[b], Abbas Hassan[c], Abdul Sadiq[d], Muhammad Saeed Jan[d], Farhan A. Khan[a], Farhat Ullah[d], Haseen Ahmad[c], Maria Bibi[a], Tariq Mahmood[a], Umer Rashid[a,*]

[a] Department of Chemistry, COMSATS University Islamabad, Abbottabad Campus, 22060, Pakistan
[b] Department of Chemistry, Hazara University, Mansehra 21120, Pakistan
[c] Department of Chemistry, Quaid-i-Azam University, Islamabad 45320, Pakistan
[d] Department of Pharmacy, University of Malakand, Chakdara 18000 Dir (L), Pakistan

ARTICLE INFO

Keywords:
Dual binding site inhibitors
Tricyclic fused rings
Desloratadine
Nonclassical AChE function
Butyrylcholinesterase

ABSTRACT

Due to recently discovered non-classical acetylcholinesterase (AChE) function, dual binding-site AChE inhibitors have acquired a paramount attention of drug designing researchers. The unique structural arrangements of AChE peripheral anionic site (PAS) and catalytic site (CAS) joined by a narrow gorge, prompted us to design the inhibitors that can interact with dual binding sites of AChE. Eighteen homo- and heterodimers of desloratadine and carbazole (already available tricyclic building blocks) were synthesized and tested for their inhibition potential against electric eel acetylcholinesterase (eeAChE) and equine serum butyrylcholinesterase (*eq*BChE). We identified a six-carbon tether heterodimer of desloratadine and indanedione based tricyclic dihydropyrimidine (**4c**) as potent and selective inhibitor of eeAChE with IC_{50} value of 0.09 ± 0.003 μM and 1.04 ± 0.08 μM (for *eq*BChE) with selectivity index of 11.1. Binding pose analysis of potent inhibitors suggest that tricyclic ring is well accommodated into the AChE active site through hydrophobic interactions with Trp84 and Trp279. The indanone ring of most active heterodimer **4b** is stabilized into the bottom of the gorge and forms hydrogen bonding interactions with the important catalytic triad residue Ser200.

1. Introduction

Alzheimer disease is characterized by the acetylcholine (ACh)-mediated abrupt blockade of cortical cholinergic neuron population and the deposition of extracellular amyloid-β (Aβ) and tau proteins into plaques and neurofibrillary tangles [1–3]. The inactivation of ACh is a unique process carried out by two cholinesterases; acetylcholinesterase (AChE) and butyrylcholinesterase (BChE), resulting in release of choline and acetate [4–6]. Thus, the inhibition of both cholinesterases (acetylcholinesterase AChE and butyrylcholinesterase BChE) is found to be the only effective therapeutic approach for AD up till now. Only five drugs have been approved for its medication since 1993. Four out of five fall under the class cholinesterase inhibitors (ChEIs): i.e. tacrine (1), donepezil (2), rivastigmine (3) and galantamine (4). Only one drug memantine (5) is an *N*-methyl-D-aspartate (NMDA) antagonist [1,7,8]. More disappointing fact is that all the current drugs, approved for AD treatment lack the disease-modifying abilities, and are mainly symptomatic. None of the approved AD drug have the ability to revert the damage or at least slow down the disease progression [9].

It is evident in some earlier studies that the ligands bind with peripheral anionic site (PAS) of AChE e.g. propidium, prevented AChE-induced Aβ aggregation. This non-classical or non-cholinergic function is distinct from active site inhibitors [10–12]. Due to this non-classical AChE function, dual binding-site AChE inhibitors have acquired a paramount attention of medicinal chemistry and drug designing researchers due to increased number of ligand-target interactions. Dual binding site inhibitors interacted with both the catalytic anionic site (CAS) at the bottom of the gorge (Trp84), and with the peripheral anionic site (PAS), near its entrance (Trp279), *via* aromatic π-staking interactions [13,14]. Donepezil shows dual-binding site interactions among FDA approved AChEIs [15]. Dual binding site inhibitors must have some structural moieties that can enter the gorge and can interact with the aromatic residues of CAS linked through a linker or a spacer that lies in the neck which is a narrow part of active site of AChE and other side of a molecule interact with amino acid residues present in PAS. Dual binding site inhibitors can be analogues, hybrids and homodimers or hetero-dimers linked through different linkers [16–23].

Tacrine (**1**), composed of a tricyclic fused ring system, is a potent

* Corresponding author.
E-mail address: umerrashid@ciit.net.pk (U. Rashid).

https://doi.org/10.1016/j.bioorg.2018.10.035
Received 4 June 2018; Received in revised form 12 October 2018; Accepted 17 October 2018
Available online 23 October 2018

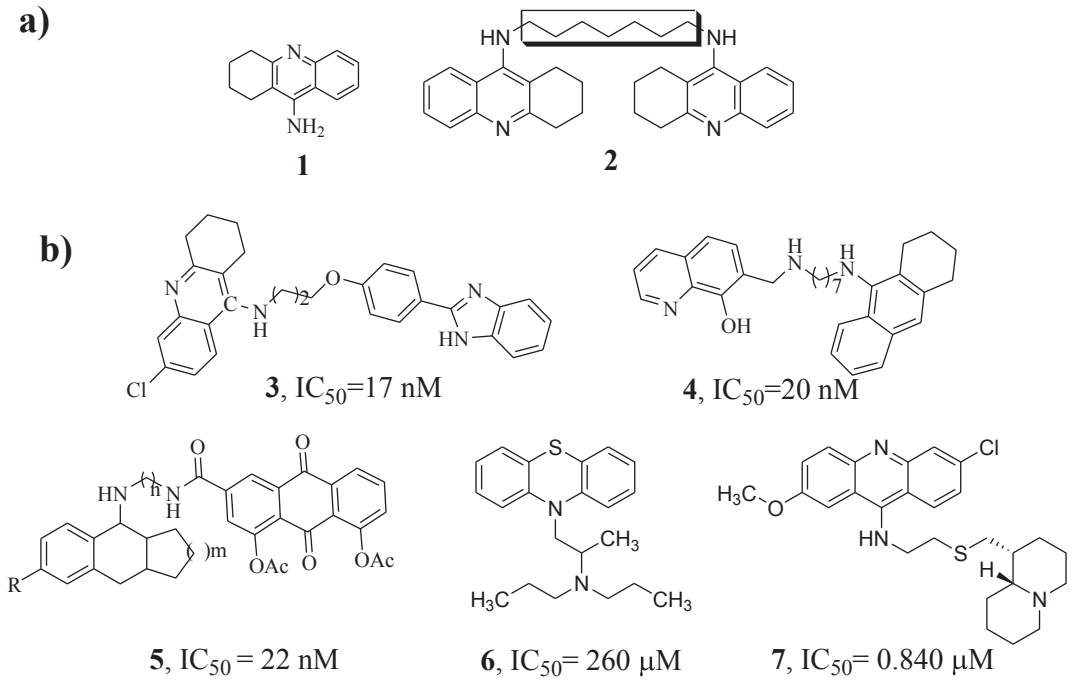

Fig. 1. (a) Tricyclic fused ring antidepressants; (b) tricyclic fused ring inhibitors of AChE.

AChE inhibitor with its potency in submicromolar range. *Bis*-tacrine (**2**) is novel compound consisting of homodimer of tacrine with heptylene linker reported as dual binding site inhibitor. Many tricyclic fused ring systems has been reported in literature as potent AChE/BChE inhibitors. Apart from tacrine and physostigmine analogues, quinolizidinyl analogous of *bi*- and tricyclic fused ring system with inhibition of ChEs in submicromolar range [24]. Tin et al. reported multipotent derivatives of phenothiazine and phenoselenazine targeting cholinergic, oxidative stress and amyloid pathways [25]. The structures of the potent tricyclic systems are shown in Fig. 1.

Recently, our group has reported dihydropyrimidine and quinazoline, a bicyclic fused ring system, based AChE and BChE inhibitors [16,26,27]. In continuation of our previous work, series of tricyclic fused ring system-based homo- and hetero-bivalent inhibitors was designed to monitor the dual binding site interactions into the AChE active site gorge. To this end, we planned to use already available tricyclic fused systems; desloratadine (**8**) and carbazole (**9**) in order to improve binding interactions. Desloratadine (**8**) is an aromatic drug having a benzene and pyridine ring fused with a seven membered cyclic ring. A piperidine ring is also present connected with a seven membered ring *via* a double bond. The calculated volume of desloratadine from online software Molinspiration (http://www.molinspiration.com/cgi-bin/properties) is 283.78 A^3. It was envisioned that this ring would result in the enhanced dual binding site interactions. Desloratadine is considered as potent antihistamine. Structural modification of desloratadine resulted in many compounds having antihistaminic and anti-inflammatory, antagonist of arginine vasopressin V2 [28,29]. On the other hand, the effect of a relatively small tricyclic carbazole (**9**, Volume = 157.01 A^3) was also investigated. Carbazole contains a fused ring system with two benzene rings fused on either side with a five membered nitrogen-heterocycle (see Fig. 2).

2. Results and discussion

2.1. Chemistry

2.1.1. Synthesis of benzyl/benzoyl derivatives of desloratadine

Benzyl derivatives of desloratadine **(1a-e)** were synthesized by reaction of desloratadine (**8**) with substituted benzyl chlorides (**10–13**) and 4-chlorobenzoyl chloride (**14**) in the presence of triethylamine as base and THF as solvent as shown in Scheme 1.

2.1.2. Synthesis of homodimers of desloratadine and carbazole

We synthesized homo- and heterodimers of selected tricyclic fused rings containing drug(s) (desloratadine)/carbazole using suitable linkers (rigid and flexible) (Schemes 2 and 3). In general strategy, for the synthesis of homodimers, 2 equivalents of desloratadine (**8**) or carbazole (**9**) were reacted with reactants **15–19** to yield **2a-e** and **3a-e** (Scheme 2). Mannich bases **2a** and **3a** were synthesized by using 2 equivalents of **8** or **9** and formalin (**15**, 40%) in ethanolic solution at room temperature. While, for the synthesis of **2b-e** and **3b-e**, desloratadine and carbazole were reacted with each of bromoacetyl bromide (**16**), dibromo- (**17**), diiodo hexane (**18**) and triazine (**19**) in dimethylformamide (DMF) using potassium carbonate as base at 70–80 °C (Scheme 2).

2.1.3. Synthesis of heterodimers of desloratadine

The design of desloratadine-carbazole heterodimers was carried out to analyze the effect of two diverse tricyclic systems on the binding interactions. For the synthesis of desloratadine-carbazole heterodimers, the tether length of two (rigid ethenone linker, **4a**) and six carbons flexible linker (**4b**) was selected. The reaction of desloratadine with bromoacetyl bromide (**16**) and diiodo hexane (**18**) resulted in intermediates **20** and **21** respectively. These intermediates further react with carbazole (**9**) in the presence of K_2CO_3 and DMF to give **4a** and **4b** respectively (Scheme 3).

Our initial pharmacological work to identify dihydropyrimidine (DHPM) scaffold as potent inhibitors of cholinesterases led us to design a new tricyclic building block [16]. Thus, synthesis of DHPM-based fused ring system (**25**) was planned through reaction of 1,3-indanedione (**22**) as a 1,3-dicarbonyl precursor in the Biginelli reaction [30]. The synthesized **25** was then reacted with intermediate **21** to synthesize target heterodimer **4c** (see Scheme 4).

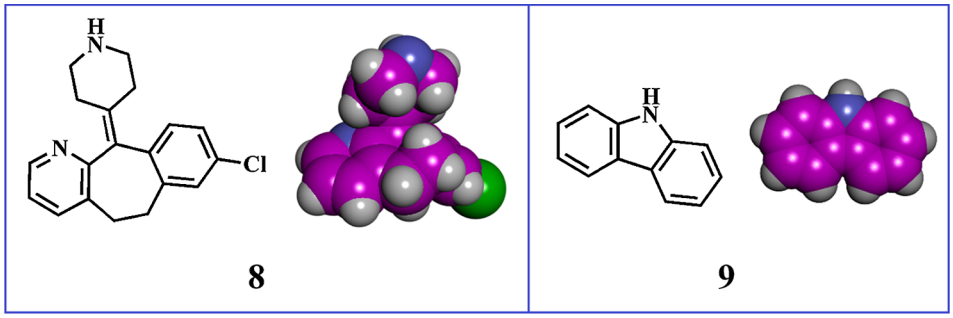

Fig. 2. Desloratadine (**8**) and carbazole (**9**) as starting structures of current research.

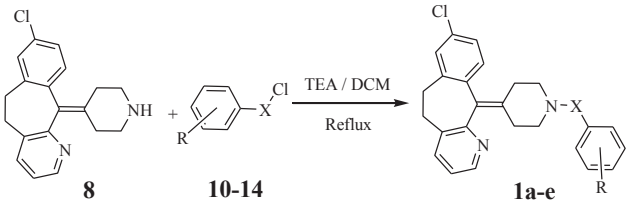

R (10-13) = -H, -4-Cl, -4-OH, -4-CH_3; X= -CH_2
R (14) = -4Cl; **X** = -C=O

Scheme 1. Synthesis of benzyl derivatives of desloratadine **(1a-e)**.

2.2. *In vitro eeAChE and eqBChE inhibition studies*

To investigate the potential of synthesized compounds, we evaluated their ability to inhibit cholinesterases. Spectroscopic Ellman's method was used for electric eel acetylcholinesterase (*ee*AChE) and butyrylcholinesterase from equine serum (*eq*BChE) assays. Tacrine and donepezil were used as reference compounds. The IC_{50} values of the parent desloratadine and carbazole was also determined for comparison purpose. Table 1 enlist the *in vitro* AChE and BChE inhibitory activities of the homodimers of desloratadine and carbazole as 50% inhibitory concentration (IC_{50}). The *in vitro* inhibitory data in Table 1 shows that all the benzyl derivatives of desloratadine (**1a-d**) are moderately active

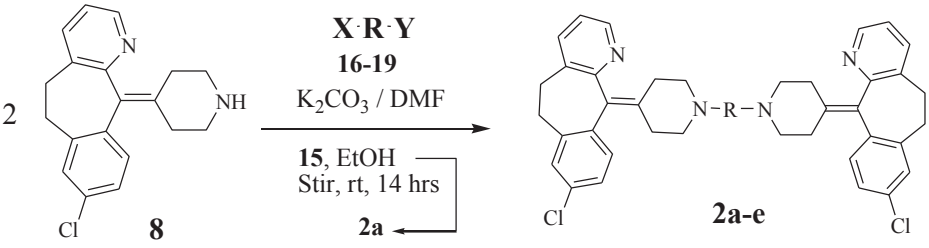

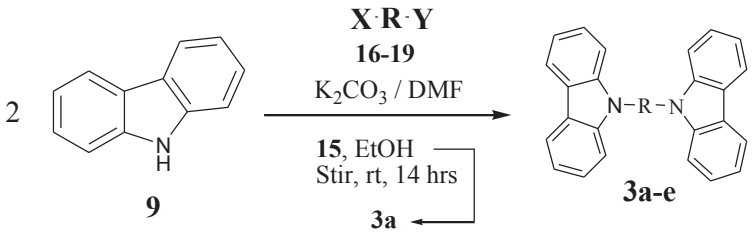

R=
2a, 3a = -CH_2-
2b, 3b = -CH_2-CO-
2c, 3c = -$(CH_2)_2$-
2d, 3d = -$(CH_2)_6$-
2e, 3e = -6-methoxy-1,3,5-triazine-

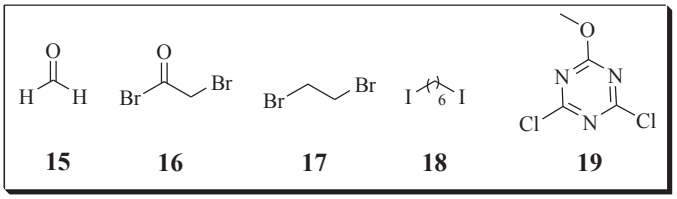

Scheme 2. Synthesis of *bis*-desloratadine (**2a-e**) from **8** and *bis*-carbazole derivatives (**3a-d**) from **9**.

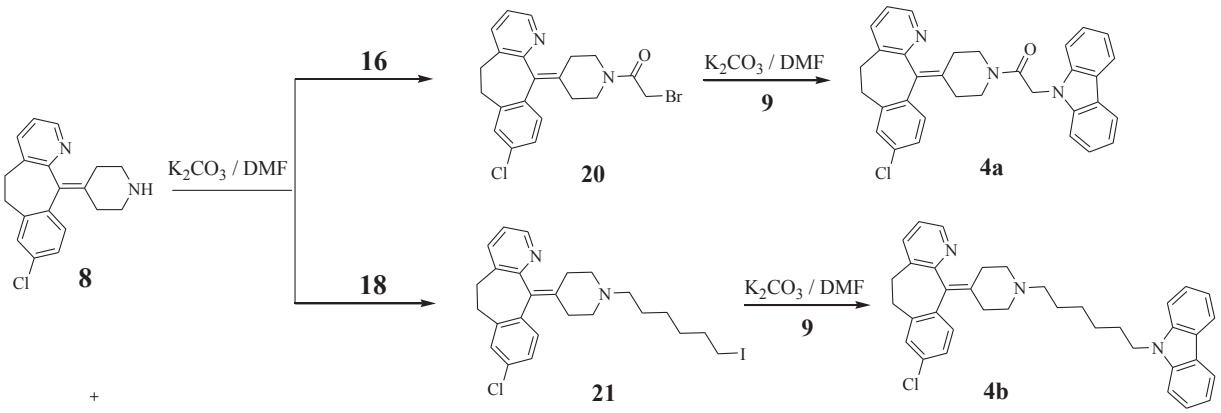

Scheme 3. Desloratadine-carbazole heterodimer **4a** and **5a**.

against AChE and showed poor inhibition for BChE. They are more active than parent desloratadine (AChE IC_{50} = 23.56 ± 0.6 μM). Benzoyl derivative **1e** has shown good inhibition with IC_{50} value of 9.51 ± 1.04 μM for AChE. Its IC_{50} value for BChE inhibition is 33.4 ± 1.28 μM.

Homodimers of desloratadine **2a-e** were emerged as potent inhibitors of AChE in low micromolar to submicromolar range. Alkylene-linked *bis*-desloratadine (**2d**, 6 carbon linker) with IC_{50} value of 0.19 ± 0.01 μM emerged as the most potent AChE inhibitor of this series. Compound **2d** is found 38.66 times more selective for AChE than BChE (IC_{50} for BChE = 7.2 ± 0.18 μM). The inhibitory data in Table 1 revealed shortening of linker length led to decrease in activity. Compound **2a** with methylene linker exhibited the potency of 6.1 ± 0.71 μM. Compounds **2b** and **2c** with linker length of two carbon atoms showed varying potency. Compound **2b** with ethanone linker exhibited the potency of 6.43 ± 0.1.19 μM. While, ethylene linker containing compound **2c** showed the potency of 1.5 ± 0.88 μM. Compound **2e** with a rigid triazine linker have shown inhibitory potential with IC_{50} value of 6.6 ± 0.43 μM. All of these compounds also showed high selectivity for AChE than BChE.

In contrast, homodimers of carbazole **3a-e** with almost same linker length were found to have moderate *ee*AChE inhibition except **3c** and **3d**. In contrast to desloratadine homodimer with the linker length of 6-carbon (**2d**), carbazole homodimer with same linker length (**3d**) showed 11 times less potency (IC_{50} = 2.1 ± 0.09 μM). All the compounds of this series also exhibited poor BChE inhibition (Table 1).

In the heterodimeric series (**4a-c**), a different influence of tricyclic system was observed. In homodimer series of desloratadine, compound **2b** with ethanone linker was almost 4 times potent than *bis*-carbazole **3b** (Table 1). The inhibition data for compounds **4a-c** in Table 1 showed that desloratadine-carbazole dimer (**4a**) with same spacer length showed IC_{50} value of 3.98 μM. The biological profile displayed by heterodimer **4b** (IC_{50} = 0.10 μM) have shown the influence of the combination of small and large ring system. The observed activity of **4b** is 1.8 and 20 times more potent than respective homodimers (**2d** and **3d** in Table 1). The most striking result of present research is the inhibition data of **4c** for both the tested enzymes. The introduction of indanone tricyclic ring lead to the most potent inhibitor of eeAChE (IC_{50} = 0.09 μM) and eqBChE (IC_{50} = 1.04 μM).

2.3. Docking study

Docking study was carried out with Molecular Operating Environment (MOE. *v*2016.08) software [31]. Only three *apo*-crystal structures of *Electrophorus electricus* acetylcholinesterase (*ee*AChE) are present in protein data bank (PDB); 1C2O, 1C2B and 1EEA with a resolution between 4.20 and 4.50 Å. In contrast, there are a number of crystal structures for *Torpedo californica* AChE (*Tc*AChE) with native ligands and good resolution. For current study, we selected 2CKM (Resolution 2.15 Å) with alkylene-linked *bis*-tacrine (7 carbon linker) as native ligand. Before the prediction of the docking poses of the synthesized compounds, we evaluated the docking reliability by re-docking of native ligand AA7 (*bis*-tacrine). The computed RMSD value of 0.892 Å was found within the acceptable criteria (< 2 Å). The binding mode analysis of the highly active compounds revealed that they bind in the active site of TcAChE almost similar to the bound inhibitor *bis*-

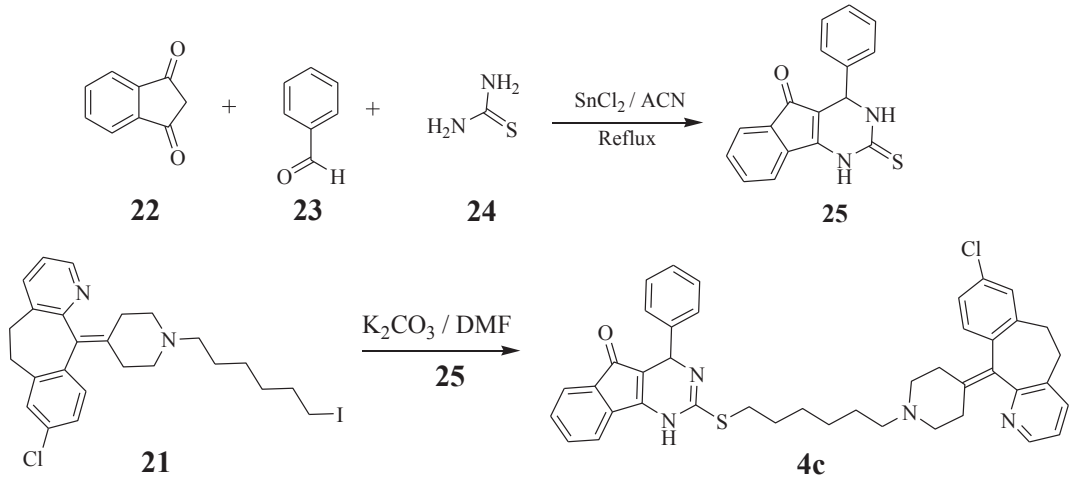

Scheme 4. Synthesis of heterodimer 4-(4-methoxyphenyl)-2-thioxo-3,4-tetrahydro-5H-indeno[1,2-*d*]pyrimidin-5-one and desloratadine (**4c**).

Table 1
ChEIs inhibition data of compounds homo- and heterodimers of desloratadine and carbazole **1a-e**, **2a-e, 3a-d** and heterodimer of desloratadine **4a-c**.

Compound	Structures	IC_{50} (μM ± SEM)		Selectivity index[a]
		eeAChE	eqBChE	
1a	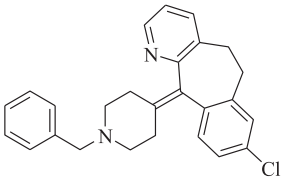	13.2 ± 0.78	118.5 ± 2.15	9.0
1b	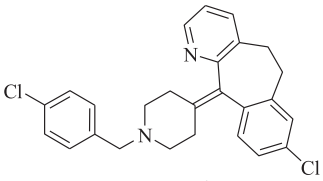	16.8 ± 0.71	121.3 ± 1.63	7.2
1c	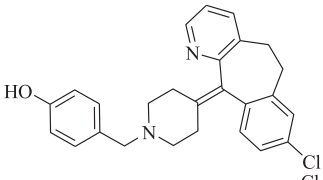	19.3 ± 1.09	109.4 ± 1.38	5.7
1d	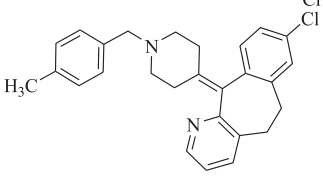	23.1 ± 1.04	103.4 ± 1.71	4.5
1e	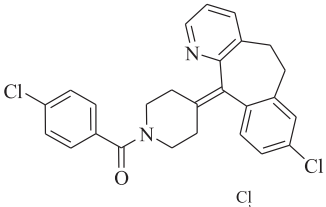	9.51 ± 1.04	33.4 ± 1.28	3.5
2a	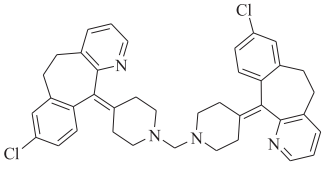	6.1 ± 0.71	55.5 ± 1.21	9.1
2b	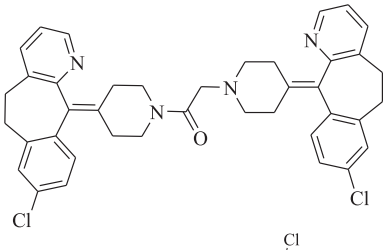	6.4 ± 1.19	51.1 ± 1.11	8.0
2c	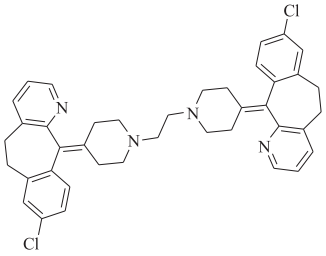	1.5 ± 0.88	12.0 ± 1.02	8.0

(*continued on next page*)

Table 1 (*continued*)

Compound	Structures	IC_{50} (μM ± SEM)		Selectivity index[a]
		eeAChE	eqBChE	
2d	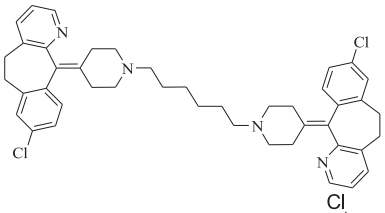	0.19 ± 0.01	7.2 ± 0.18	38.0
2e	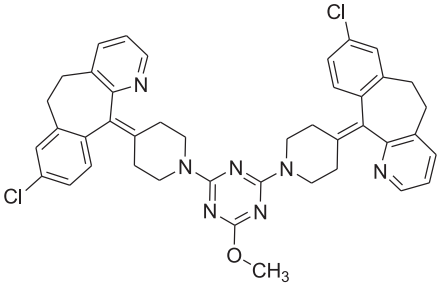	6.6 ± 0.43	75.1 ± 1.23	11.4
3a	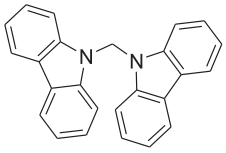	34.9 ± 1.61	80.2 ± 1.76	2.3
3b	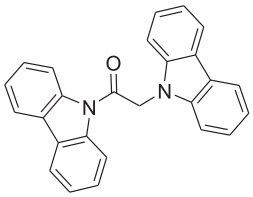	25.4 ± 1.98	112.2 ± 1.43	4.4
3c	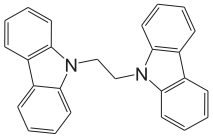	7.3 ± 1.10	98.2 ± 2.04	13.4
3d	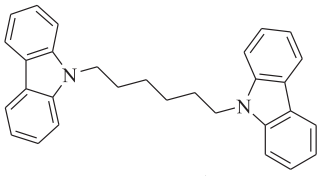	2.1 ± 0.09	39.5 ± 1.36	18.1
3e	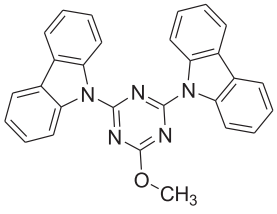	13.4 ± 1.65	45.0 ± 1.64	3.3
4a	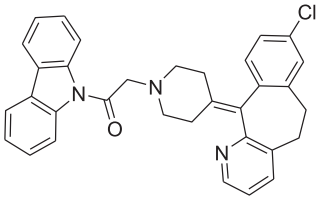	4.0 ± 0.58	48.6 ± 1.37	12.1

(*continued on next page*)

Table 1 (*continued*)

Compound	Structures	IC_{50} (μM ± SEM)		Selectivity index[a]
		eeAChE	eqBChE	
4b	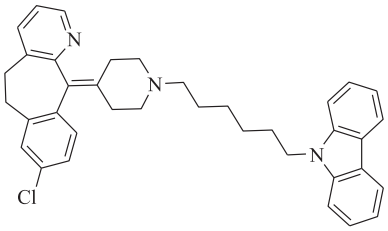	0.10 ± 0.009	4.3 ± 0.08	43.0
4c	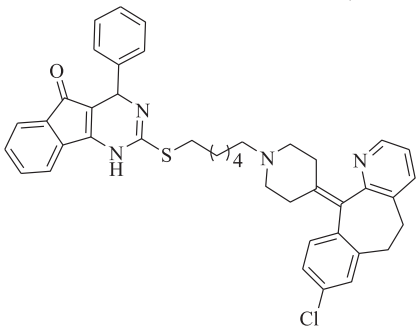	0.09 ± 0.003	1.04 ± 0.08	11.1
Desloratadine		23.6 ± 0.56	34.1 ± 0.81	1.4
Carbazole		58.6 ± 1.68	110.3 ± 2.3	1.8
Donepezil		**0.05 ± 0.01**	**5.4 ± 0.27**	108.0
Tacrine		**0.4 ± 0.019**	**0.06 ± 0.009**	0.15

[a] Selectivity Index = IC_{50} of BChE/IC_{50} of AChE.

tacrine (B7T). The overlaid binding poses of bis-desloratadine homodimers **2c and 2d** with **B7T** are shown in Fig. 3a–c. They all are engaged in π-π stacking interactions with aromatic residues of Trp84 and Trp279. The molecular modeling results suggest that the most potent inhibitor (**2d,** IC_{50} = 0.187 ± 0.71) of the series 2 was docked on *Tc*AChE, resulting in almost similar binding pose to B7T. The inhibitor is well inserted into the binding groove extending from bottom of the gorge to PAS (Fig. 4a–b). It interacts simultaneously with PAS and CAS residues. One of the tricyclic desloratadine ring of the homodimer bound to CAS of *ee*AChE and forms π-π stacking interactions with Trp84 and Phe330. The other tricyclic desloratadine ring is bound to the PAS and interacts with Tyr70 and Trp279 (Fig. 4c). For compound **2c** bearing a shorter flexible linker (dimethylene), one of the tricyclic ring located in CAS and by interacting with Trp84 and Phe330. While, the other ring interacts with Trp279 through hydrogen bonding with pyridine nitrogen of desloratadine (Fig. 4d–e).

Carbazole homodimers have shown moderate to poor inhibition potential against eeAChE. The most active homodimer of carbazole is **3d** with hexamethylene linker (IC_{50} = 2.07 ± 0.09 μM). Tricyclic carbazole ring inserted into the CAS and interacts with Trp84 at a distance of 3.81 Å and with Phe330 (3.87 Å). Heterodimers (**4a–c**) also showed similar binding orientation to that of B7T. The lowest-energy docking poses of **4b** and **4c** are shown in Fig. 5a–b. The docking pose of compound **4b** is shown in Fig. 5a. Desloratadine and carbazole rings forms strong π-π stacking interactions with Phe330, Trp84 and Tyr70, Trp279 respectively. Small tricyclic ring, carbazole, is accommodated

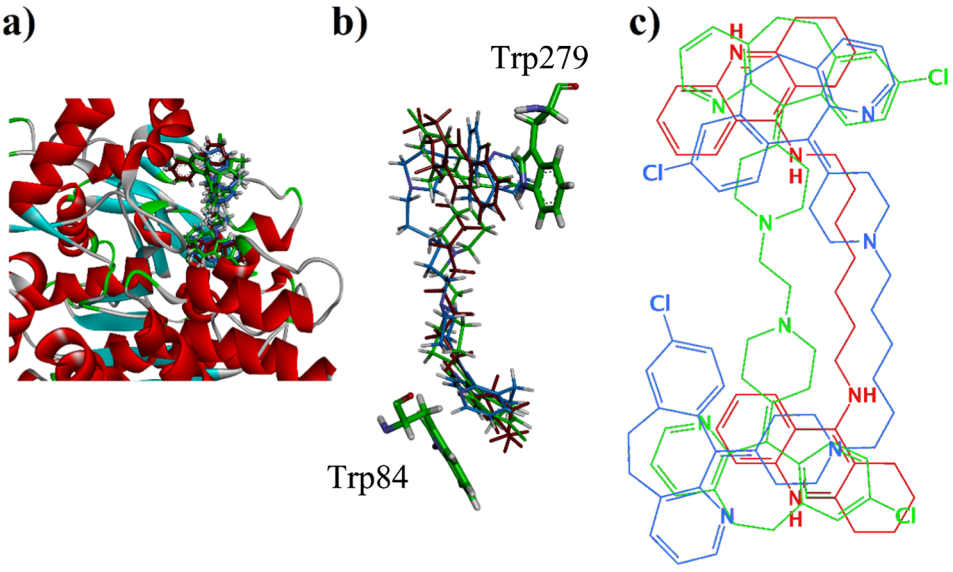

Fig. 3. (a) The overlaid ribbon diagram of **B7T, 2c** and **2d** into the binding site of TcAChE (2CKM). (b) Close-up 3-D depiction of superimposed bound conformations (line-model) of; **B7T** (red), **2c** (green) and **2d** (blue). The key residues (Trp84 and Trp279) are shown in green sticks. (c). Two-dimensional (2-D) depiction of superimposed ligands (generated by MOE).

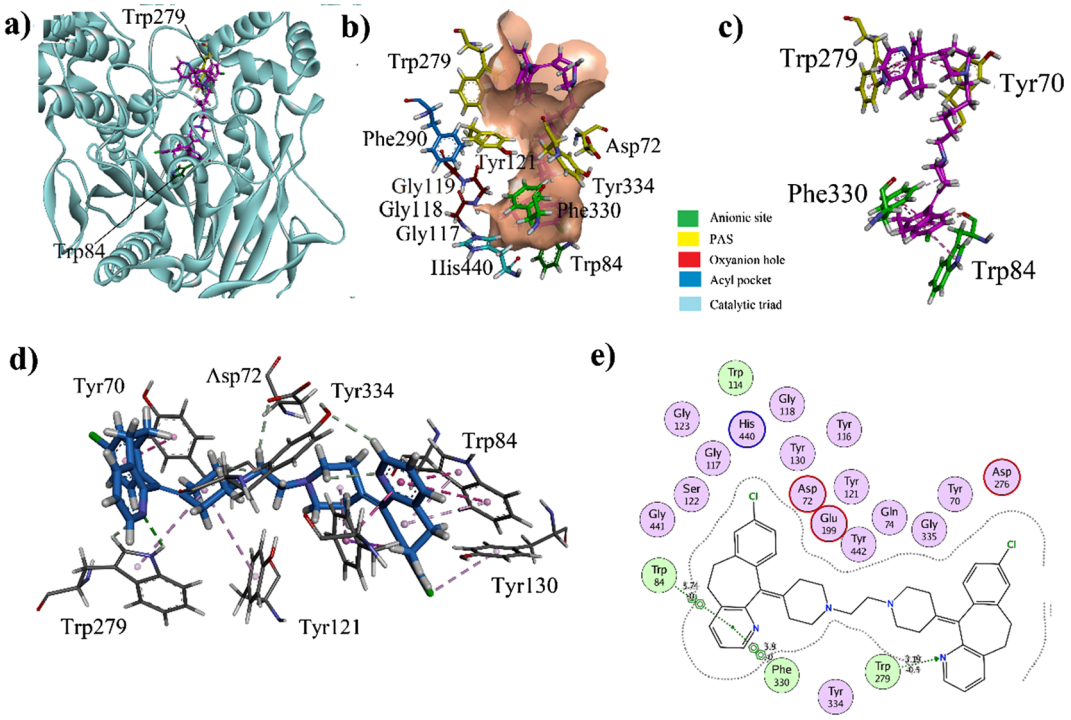

Fig. 4. (a–c) Three-dimensional (3-D) docking poses of compound **2d** into the active site of **2CKM**. (a) Ribbon diagram; (b) Stick model. The active site residues are depicted in colored sticks. (c) Close-up view of the docked-pose of **2d** showing important residues. (d–e) Lowest-energy docking pose of **2e** into the active site (d) 3-D close-up view, (e) 2-D interaction plot.

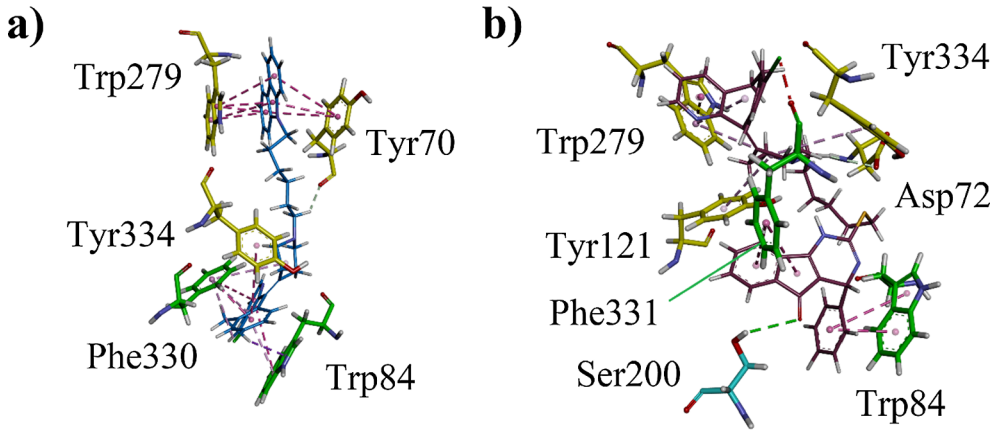

Fig. 5. Close-up depiction of the lowest-energy three-dimensional (3-D) docking poses of compounds (a) **4b** and (b) **4c**.

in PAS region and forms π-π stacking interactions with Tyr70 and Trp279. On the other hand, the docking pose of the most potent compound of current research **4c** establishes hydrogen bonding as well as π-π stacking interactions with the key residues (Fig. 5b). The tricyclic indanone ring is well accommodated into the bottom of the gorge and its carbonyl oxygen forms hydrogen bonding interactions with the important catalytic triad residue Ser200. While, phenyl ring at 4-position forms π-π stacking interactions with Trp84. The binding mode of important compounds are shown in Figs. S-1 to S-7 (Supplementary information).

3. Conclusions

Alzheimer disease is a brain disorder. Many inhibitors have been synthesized until now to the cope the disease and only symptoms are controllable by the already available drugs in market. This study aimed to design and synthesize some dual binding site (DBS) inhibitors and test their activity against AChE/BChE. A series of 18 compounds were designed and synthesized having tricyclic fused ring systems. The salient features from the *in vitro* AChE/BChE inhibition data can be summarized as follows: Parent compounds desloratadine and carbazole exhibited poor AChE and BChE inhibition. Benzyl/benzoyl derivatives of desloratadine (**1a-e**) also showed poor inhibition of both enzymes. Tricyclic homodimers of desloratadine emerged as potent inhibitors compared with the carbazole derivatives. Flexible methylene (ethyl or hexyl) homodimers (Table 1**, 2c, 2d and 3d**) showed excellent AChE inhibition but poor selectivity for BChE. Highly rigid triazine showed good to moderate AChE inhibition. Rigid ethenone linker (**2b** and **3b**) showed less inhibition than slightly flexible ethyl linker (**2c** and **3c**). Indanedione tricyclic heterodimer of desloratadine (**4c**) with a six-carbon tether displayed nanomolar potency. Binding pose analysis of potent inhibitors suggest that tricyclic ring is well accommodated into the AChE active site through hydrophobic interactions with Trp84 and Trp279. The indanone ring of most active heterodimer **4b** is stabilized

into the bottom of the gorge and forms hydrogen bonding interactions with the important catalytic triad residue Ser200.

4. Material and methods

4.1. General

All the reagents and solvents were purchased from standard commercial vendors and were used without any further purification. Desloratadine and carbazole were purchased from Sigma Aldrich. ^{1}H and ^{13}C NMR spectra were recorded in deuterated solvents on a Bruker spectrometer at 300 and 75 MHz respectively using tetramethylsilane (TMS) as internal reference. Chemical shifts are given in δ scale (ppm). Melting points were determined in open capillaries using Gallen Kamp melting point apparatus (MP-D). The progress of all the reactions was monitored by TLC on 2.0 × 5.0 cm aluminum sheets pre-coated with silica gel 60F254 with a layer thickness of 0.25 mm (Merck). LC-MS spectra were obtained using Agilent technologies 1200 series high performance liquid chromatography comprising of G1315 DAD (diode array detector) and ion trap LCMS G2445D SL. HPLC analysis were carried out on Schimadzu LC20AT. Elemental analyses were conducted using a LECO-932 CHNS Analyzer (LECO Corporation, USA).

4.2. General procedure for synthesis of benzyl/benzoyl derivatives of desloratadine (1a-e)

To solution of desloratadine (**8**, 10 mmol) in dichloromethane (DCM, 30 mL) added Et_3N and stirred at 0 °C for 10–15 min. To this solution, 10 mmol of benzyl/benzoyl bromide (**21–25**) dissolved in 15 mL of DCM was added drop-wise and then heated to reflux until the completion of reaction (TLC). After the completion of reaction, mixture was poured into ice, filtered and recrystallized from ethanol.

4.2.1. 11-(1-benzylpiperidin-4-ylidene)-8-chloro-6,11-dihydro-5H-benzo [5,6]cyclohepta[1,2-b]pyridine (1a)

1a was synthesized according to general procedure by using **8** and benzyl chloride **(21)**. R_f 0.44 (*n*-hexane/ethyl acetate 6:1). Yield 73%, m.p. 156–155 °C. ^{1}H NMR (300 MHz, $CDCl_3$): δ 8.39 (d, 1H, J = 7.5 Hz, Ar-*H*), 7.48 (d, 1H, J = 7.8 Hz, Ar-*H*), 7.20–7.15 (m, 4H, Ar-*H*), 7.10–7.06 (m, 5H, Ar-*H*), 3.66 (s, 2H, CH_2), 3.10–3.01 (m, 2H, CH_2), 2.83–2.73 (m, 2H, CH_2), 2.61–2.59 (m, 2H, CH_2), 2.40–237 (m, 2H, CH_2), 2.18–2.08 (m, 4H, 2 × CH_2); ^{13}C NMR (75 MHz, $CDCl_3$): 153.2, 143.9, 137.5, 136.4, 133.5, 133.2 (2C), 132.2, 129.9, 126.6 (2C), 126.2 (2C), 124.5, 124.2 (2C), 123.7, 117.7, 114.2, 62.5, 57.5 (2C), 31.7 (2C), 29.9, 28.2.

4.2.2. 8-chloro-11-(1-(4-chlorobenzyl) piperidin-4-ylidene)-6, 11-dihydro-5H-benzo[5,6]cyclohepta [1, 2-b] pyridine (1b)

1b was synthesized according to general procedure by using **8** and 4-chlorobenzylchloride **(22)**. R_f 0.55 (*n*-hexane/ethyl acetate 6:1). Yield 74%, m.p. 158–161 °C. ^{1}H NMR (300 MHz, $CDCl_3$): δ 8.39 (d, 1H, J = 7.5 Hz, Ar-*H*), 7.38 (d, 1H, J = 7.8 Hz, Ar-*H*), 7.14–7.06 (m, 8H, Ar-*H*), 3.68 (s, 2H, CH_2), 2.79–2.70 (m, 4H, 2 × CH_2), 2.45–2.25 (m, 8H, 4 × CH_2); ^{13}C NMR (75 MHz, $CDCl_3$): 153.1, 143.9, 137.3, 134.5, 133.2, 132.9 (2C), 132.0, 130.6, 129.0 (2C), 126.3 (2C), 124.6, 124.2 (2C), 123.8, 117.7, 114.0, 62.4, 57.6 (2C), 31.7 (2C), 30.1, 28.4.

4.2.3. 4-((4-(8-Chloro-5H-benzo[5,6]cyclohepta[1,2-b]pyridin-11(6H)-ylidene)piperidin-1-yl)methyl)phenol (1c)

1c was synthesized according to general procedure by using **8** and 4-hydroxybenzylchloride **(23)**. R_f 0.48 (*n*-hexane/ethyl acetate 6:1). Yield 63%, m.p. 160–163 °C. ^{1}H NMR (300 MHz, $CDCl_3$): δ 9.88 (brs, 1H, –OH), 8.42 (d, 1H, Ar-*H*), 7.48 (d, 1H, Ar-*H*), 7.18 (m, 4H, Ar-*H*), 6.98 (d, 2H, Ar-*H*), 6.74 (d, 2H, Ar-*H*), 3.63 (s, 2H, CH_2), 3.04–2.96 (m, 2H, CH_2), 2.81–2.74 (m, 2H, CH_2), 2.61–2.55 (m, 2H, CH_2), 2.46–2.39 (m, 2H, CH_2), 2.14–2.08 (m, 4H, 2 × CH_2); ^{13}C NMR (75 MHz, $CDCl_3$): 153.3, 153.0, 144.1, 137.6, 133.4, 133.0 (2C), 131.1, 129.9, 128.8 (2C), 124.9 (2C), 123.9, 123.6, 118.1, 114.2, 113.4 (2C), 62.8, 57.4 (2C), 31.8 (2C), 30.1, 28.8.

4.2.4. 8-chloro-11-(1-(4-methylbenzyl) piperidin-4-ylidene)-6, 11-dihydro-5H-benzo[5,6,]cyclohepta [1,2-b] pyridine (1d)

1d was synthesized according to general procedure by using **8** and 4-methylbenzylchloride **(24)**. R_f 0.52 (*n*-hexane/ethyl acetate 6:1). Yield 72%, m.p. 171–173 °C. ^{1}H NMR (300 MHz, $CDCl_3$): δ 8.40 (d, 1H, J = 7.2 Hz, Ar-*H*), 7.46 (d, 1H, J = 7.8 Hz, Ar-*H*), 7.18 (m, 4H, Ar-*H*), 7.06 (d, 2H, Ar-*H*), 6.94 (d, 2H, Ar-*H*), 3.63 (s, 2H, CH_2), 2.99–2.89 (m, 2H, CH_2), 2.75–2.68 (m, 2H, CH_2), 2.58–2.52 (m, 2H, CH_2), 2.45–2.39 (m, 2H, CH_2), 2.27 (s, 3H, CH_3), 2.14–2.08 (m, 4H, 2 × CH_2); ^{13}C NMR (75 MHz, $CDCl_3$): 154.0, 143.6, 137.5, 134.7, 133.5, 133.2 (2C), 131.9, 129.8 (2), 128.8 (2C), 126.5 (2C), 125.5, 125.2, 123.5, 117.7, 114.2, 62.5, 57.3 (2C), 31.5 (2C), 30.1, 28.5, 22.3.

4.2.5. 13-chloro-2-[1-(4-chlorobenzoyl)piperidin-4-ylidene]-4-azatricyclo [9.4.0.0^{3,8}]penta- deca-1(15),3(8),4,6,11,13-hexaene (1e)

1e was synthesized according to general procedure by using **8** and 4-chlorobenzoyl chloride (**25**). R_f = 0.35 (*n*-hexane/ethyl acetate 6:1). Yield 76%, m.p. 210–212 °C. ^{1}H NMR (300 MHz, $CDCl_3$): δ 8.56 (d, 1H, J = 7.5 Hz, Ar-*H*), 7.86 (d, 2H, J = 8.1 Hz, Ar-*H*), 7.51 (d, 1H, J = 7.5 Hz, Ar-*H*), 7.36 (d, 2H, J = 8.1 Hz, Ar-*H*), 7.19–7.11 (m, 4H, Ar-*H*), 3.37–3.28 (m, 4H, CH_2), 2.78–2.69 (m, 2H, CH_2), 2.31–2.22 (m, 2H, CH_2), 2.00–1.95 (m, 4H, 2 × CH_2); ^{13}C NMR (75 MHz, $CDCl_3$): 170.2, 153.8, 143.7, 137.4, 134.0, 133.4, 132.9 (2C), 132.0, 129.5, 129.0, 127.6 (2C), 126.4 (2C), 124.9, 123.6, 117.5, 114.0, 47.3 (2C), 31.7 (2C), 29.9.

4.3. General procedure for the synthesis of desloratadine and carbazole derivatives 2a and 3a

To a solution of one equivalent of desloratadine (**8**, 10 mmol) or carbazole (**9**) in ethanol (15 mL), formalin 40% (**26**, 1.0 equiv. 10 mmol) was added and stirred for 10–15 min at room temperature. in EtOH (15 mL). A solution of another on equivalent of desloratadine (0.6 mmol) or carbazole in ethanol (5 mL) was then added drop-wise to it. The reaction was stirred and monitored by TLC to completion. The mixture was then kept overnight in refrigerator. The precipitates thus produced were filtered and recrystallized from ethanol to obtain **2a** and **3a**.

4.3.1. 13-chloro-2-{1-[(4-{13-chloro-4-azatricyclo[9.4.0.0^{3,8}] pentadeca-1(11),3(8), 4,6,12,14-hexaen-2-ylidene}piperidin-1-yl) methyl]piperidin-4-ylidene}-4-azatricyclo [9.4.0.0^{3,8}] pentadeca-1(15),3(8),4,6,11,13-hexaene (2a)

2a was synthesized according to general procedure by using **8** and formalin (**26**). Yield = 70%; m.p. 224–228 °C; R_f = 0.58 (*n*-hexane/ethyl acetate 7:1). ^{1}H NMR (300 MHz, $CDCl_3$): 8.34 (d, 2H), 7.44 (d, 2H), 7.12 (m, 8H), 3.53 (s, 2H), 3.01–2.92 (m, 4H, 2 × CH_2), 2.78–2.71 (m, 4H, 2 × CH_2), 2.63–2.58 (m, 4H, 2 × CH_2), 2.38–2.32 (m, 4H, 2 × CH_2), 2.19–2.12 (m, 4H, 2 × CH_2), 2.00–1.92 (m, 4H, 2 × CH_2). ^{13}C NMR (75 MHz, $CDCl_3$): 157.3 (2C), 144.9 (2C), 137.5 (2C), 132.5 (2C), 132.2 (4C), 132.0 (2C), 131.2 (2C), 129.0 (2C), 126.5 (2C), 126.2 (2C), 123.7 (2C), 119.7 (2C), 114.2 (2C), 87.2, 55.6 (4C), 32.4 (2C), 32.0 (2C), 29.9 (2C); LC-MS (*m/z*) [M + H+] = 633.3

4.3.2. Di(9H-carbazol-9-yl)methane (3a)

3a was synthesized according to general procedure by using **9** and formalin (**26**). Yield = 77%; R_f = 0.46 (*n*-hexane/ethyl acetate 7:1); m.p. 290–293 °C; ^{1}H NMR (300 MHz, $CDCl_3$): δ 7.54 (d, 4H, J = 7.2 Hz, Ar-*H*), 7.47 (d, 4H, J = 7.5 Hz, Ar-*H*), 7.33 (t, 4H, J = 7.5 Hz, Ar-*H*), 7.24 (t, 4H, J = 7.5 Hz, Ar-*H*), 6.50 (s, 2H, –CH_2); ^{13}C NMR (75 MHz, $CDCl_3$): 137.1 (4C), 126.0(4C), 125.4(4C), 120.4(4C), 119.8(4C), 110.0(4C), 80.1; LC-MS found for $C_{25}H_{18}N_2$ (*m/z*) = 347.2 [M + H$^+$].

*4.4. General procedure for the synthesis of homodimers of bis-desloratadine (**2b-e**) and bis-carbazole (**3b-e**)*

A mixture of desloratadine/carbazole (2.0 eq; 8.686 mmol) and K_2CO_3 (2.0 eq; 17.373 mmol) in DMF (10 mL) at 0 °C under N_2. Stirred the mixture for 20 min and then add dihalo-compounds (**27**–**30**, 1.0 eq;) in the reaction mixture drop wise at 0 °C. Then stay room temperature and maintain the temperature at 70–80 °C and reflux the mixture for 5–6 h. The reaction was monitored by TLC. The extraction was done with water and chloroform (3 times in 50 mL/10 mL ratio). Anhydrous sodium sulfate is added to dry off the mixture. The solvent was evaporated and crude was obtained. Further, crude mixture was purified by silica gel column chromatography (*n*-hexanes/ethyl acetate).

4.4.1. Synthesis of Bis-desloratadine derivatives (2b-e)

4.4.1.1. 2-(4-{13-chloro-4-azatricyclo[9.4.0.0^{3,8}]pentadeca-1(11),3(8),4,6,12,14-hexaen-2-ylidene} piperidin-1-yl)-1-(4-{13-chloro-4-azatricyclo[9.4.0.0^{3,8}]pentadeca-1(15),3(8),4,6,11,13-hexaen-2-ylidene}piperidin-1-yl)ethan-1-one (2b). **2b** was synthesized according to general procedure by using **8** and bromoacetyl bromide (**27**). Purified by silica gel column chromatography (*n*-hexanes/ethyl acetate 5:1). Yield = 69%; R_f = 0.43 (*n*-hexane/ethyl acetate 7:1); m.p. 215–219 °C; ^{1}H NMR (300 MHz, $CDCl_3$): δ 8.29 (d, 2H, *J* = 4.2 Hz, Ar-*H*), 7.43 (d, 2H, *J* = 6.9 Hz, Ar-*H*), 7.09–7.01 (m, 8H), 3.43–3.20 (m, 4H), 3.16 (t, 4H, *J* = 12.6 Hz), 3.01 (s, 2H), 2.88–2.76 (m, 8H), 2.59–2.35 (m, 8H). ^{13}C NMR (75 MHz, $CDCl_3$): 163.9, 157.4 (2C), 145.1 (2C), 137.6 (2C), 134.5 (2C), 134.0 (4C), 133.4 (2C), 131.6 (2C), 131.1 (2C), 129.1 (2C), 126.5 (2C), 126.0 (2C), 123.4 (2C), 119.6 (2C), 114.1 (2C), 57.9 (2C), 55.5, 46.5 (2C), 32.4 (2C), 32.0 (2C), 30.1 (2C). LC-MS found for $C_{40}H_{38}Cl_2N_4O$ (*m/z*) = 661.2 [M + H].

4.4.1.2. 13-chloro-2-{1-[2-(4-{13-chloro-4-azatricyclo[9.4.0.0^{3,8}] pentadeca-1(11),3(8),4,6,12,14-hexaen-2-ylidene}piperidin-1-yl)ethyl] piperidin-4-ylidene}-4-azatricyclo[9.4.0.0^{3,8}] pentadeca-1(15),3(8),4,6, 11,13-hexaene (2c). **2c** was synthesized according to general procedure by using **8** and 1,2-dibromoethane (**28**). Yield = 71%; R_f = 0.58 (*n*-hexanes/ethyl acetate 5:1); m.p. 250–254 °C; ^{1}H NMR (300 MHz, $CDCl_3$, TMS): δ 8.40 (d, 2H), 7.43 (m, 2H), 7.34 (m, 2H, Ar-*H*), 7.33 (m, 2H, Ar-*H*), 7.28 (m, 2H, Ar-*H*), 6.98 (m, 2H,), 3.08–3.00 (m, 4H), 2.83–2.75 (m, 4H), 2.65–2.56 (m, 4H), 2.48 (t, 4H, *J* = 7.2 Hz, $2CH_2$), 2.41–2.34 (m, 4H), 2.21–2.14 (m, 8H), ^{13}C NMR (75 MHz, $CDCl_3$): δ 157.3 (2C), 144.8 (2C), 137.5 (2C), 132.3 (2C), 132.1 (4C), 131.9 (2C), 130.0 (2C), 129.0 (2C), 126.6 (2C), 126.1 (2C), 123.5 (2C), 119.7 (2C), 114.0 (2C), 55.0 (4C), 52.9 (2C), 32.1 (2C), 31.8 (2C), 29.8 (2C). LC-MS found for $C_{40}H_{40}Cl_2N_4$ (*m/z*) $[M+H]^+$ = 647.3.

4.4.1.3. 13-chloro-2-{1-[6-(4-{13-chloro-4-azatricyclo[9.4.0.0^{3,8}] pentadeca1 (11),3(8), 4,6, 12,14-hexaen-2-ylidene}piperidin-1-yl)hexyl] piperidin-4-ylidene}-4-azatricyclo [9.4.0.0^{3,8}]pentadeca-1(15),3(8),4,6, 11,13-hexaene (2d). **2d** was synthesized according to general procedure by using **8** and 1,6-diiodohexane (**29**). Yield = 74%; Rf = 0.55 (*n*-hexanes/ethyl acetate 6:1); m.p. 241–245 °C; 1H NMR (300 MHz, $CDCl_3$, TMS): 8.48–8.46 (m, 2H, Ar-H), 7.54 (d, 2H, *J* = 7.8 Hz, Ar-H), 7.19–7.05 (m, 8H, Ar-H), 3.01–2.83 (m, 8H), 2.41–2.32 (m, 12H), 2.11–2.00 (m, 8H), 1.44–1.35 (m, 8H); ^{13}C NMR (75 MHz, $CDCl_3$): 158.9 (2C), 147.2 (2C), 140.5 (2C), 136.1 (2C), 135.8 (4C), 135.5 (4C), 131.2 (2C), 129.5 (2C), 129.4 (2C), 128.5 (2C), 122.8 (2C), 115.9 (2C), 58.1 (4C), 55.0 (2C), 31.7 (4C), 29.1 (2C), 28.9 (2C), 25.9 (2C), 22.5 (2C). LC-MS found for $C_{44}H_{48}Cl_2N_4$ (*m/z*) = 703.4 [M + H].

4.4.1.4. Synthesis of 13-chloro-2-{1-[4-(4-{13-chloro-4-azatricyclo [9.4.0.0^{3,8}] pentadeca-1(11),3(8),4,6,12,14-hexaen-2-ylidene}piperidin-1-yl)-6-methoxy-1,3,5-triazin-2-yl] piperidin-4-ylidene}-4-azatricyclo [9.4.0.0^{3,8}]pentadeca-1(15),3(8),4,6,11,13-hexaene (2e). **2e** was synthesized according to general procedure by using **8** and 2, 4-dichloro-6-methoxy-1,3,5-triazine (**30**). Yield = 73%; R_f = 0.57 (*n*-hexanes/ethyl acetate 6:1); m.p. 235–237 °C; ^{1}H NMR (300 MHz, DMSO-d_6): 8.34–8.31 (m, 2H, Ar-H), 7.57–7.55 (m, 2H, Ar-H), 7.28 (d, 2H, Ar-H), 7.21–7.16 (m, 4H, Ar-H), 7.06 (d, 2H, *J* = 8.1 Hz, Ar-H), 3.84 (s, 3H, $-OCH_3$), 3.36–3.27 (m, 8H), 2.85–2.69 (m, 8H), 2.25–2.13 (m, 8H). ^{13}C NMR (75 MHz, DMSO-d_6): 178.9 (2C), 169.6, 157.6 (2C), 145.1 (2C), 137.4 (2C), 132.5 (2C), 132.1 (4C), 131.8 (2C), 131.2 (2C), 129.0 (2C), 126.4 (2C), 126.2 (2C), 123.5 (2C), 119.6 (2C), 114.2 (2C), 53.5, 52.0 (4C), 32.4 (2C), 32.0 (2C), 30.0 (2C). LC-MS for $C_{42}H_{39}Cl_2N_7O$ (*m/z*) 728.3 [M + H].

*4.4.2. Synthesis of Bis-carbazole homodimers (**3b-e**)*

*4.4.2.1. 1,2-di(9H-carbazol-9-yl)ethan-1-one (**3b**)*. **3b** was synthesized according to general procedure by using **9** and bromoacetyl bromide (**27**). Yield = 77%; R_f = 0.62 (*n*-hexanes/ethyl acetate 5:1); m.p. 290–293 °C; ^{1}H NMR (300 MHz, $CDCl_3$): 7.83 (d, 2H, *J* = 8.1 Hz, Ar-H), 7.52 (d, 2H, *J* = 7.8 Hz, Ar-H), 7.45 (d, 2H, *J* = 7.8 Hz, Ar-H), 7.33 (d, 2H, *J* = 7.5 Hz, Ar-H), 7.12–7.01 (m, 8H, Ar-H), 5.07 (s, 2H, $-CH_2$). ^{13}C NMR (75 MHz, $CDCl_3$): 198.1, 132.8 (2C), 130.3 (2C), 123.9(4C), 122.4(4C), 120.4(4C), 117.6 (2C), 117.1 (2C), 113.4(4C), 57.4; LC-MS found for $C_{26}H_{18}N_2$ (*m/z*) = 375.2 [M + H].

*4.4.2.2. 1,2-di(9H-carbazol-9-yl)ethane (**3c**)*. **3c** was synthesized according to general procedure by using **9** and 1,2-dibromoethane (**28**). Yield = 79%; R_f = 0.51 (*n*-hexanes/ethyl acetate 5:1); m.p. 299–300 °C; ^{1}H NMR (300 MHz, $CDCl_3$): 7.71 (d, 4H, *J* = 7.5 Hz, Ar-H), 7.48 (m, 8H, Ar-H), 7.25 (m, 4H, Ar-H), 4.25 (s, 4H, 2 × CH_2); ^{13}C NMR (75 MHz, $CDCl_3$): 132.7 (4C), 120.6(4C), 120.5(4C), 120.2(4C), 117.5 (4C), 108.0 (4C), 59.8 (2C). LC-MS found for $C_{26}H_{20}N_2$ (*m/z*) = 361.2 [M + H +].

*4.4.2.3. 9-(6-(9H-carbazol-9-yl)hexyl)-9H-carbazole (**3d**)*. **3d** was synthesized according to general procedure by using **9** and 1,6-diiodohexane (**18**). ^{1}H NMR (300 MHz, $CDCl_3$): 7.73 (d, 4H, *J* = 7.5 Hz, Ar-H), 7.39–7.31 (m, 8H, Ar-H), 7.17–7.10 (m, 4H, Ar-H), 4.05 (t, 4H, *J* = 6.6 Hz, CH_2), 1.91–1.80 (m, 4H, CH_2), 1.32 (t, 4H, *J* = 6.6 Hz, CH_2); ^{13}C NMR (75 MHz, CDCl3): 132.8 (4C), 120.2 (4C), 119.6 (4C), 119.4 (4C), 118.0 (4C), 107.0 (4C), 56.1 (2C), 28.2 (2C), 25.7 (2C). LC-MS found for $C_{30}H_{28}N_2$ (*m/z*) = 417.3 [M + H].

*4.4.2.4. 9,9′-(6-methoxy-1,3,5-triazine-2,4-diyl)bis(9H-carbazole) (**3e**)*. **3e** was synthesized according to general procedure by using **9** and 2, 4-dichloro-6-methoxy-1,3,5-triazine (**30**). Yield = 80%; R_f = 0.57 (*n*-hexanes/ethyl acetate 5:1); m.p. 319–321 °C; ^{1}H NMR (300 MHz, $CDCl_3$): 7.73 (d, 4H, *J* = 7.5 Hz), 7.50 (m, 8H), 7.25 (m, 4H), 3.85 (s, 3H); ^{13}C NMR (75 MHz, $CDCl_3$): 176.7 (2C), 172.8, 136.5 (4C), 124.4 (4C), 123.5 (4C), 122.2 (4C), 117.2 (4C), 107.2(4C), 52.4; LC-MS found for $C_{28}H_{19}N_5O$ (*m/z*) = 442.2 [M + H +].

4.5. Synthesis of desloratadine-carbazole hetero-dimers

*4.5.1. Synthesis of 1-(9H-carbazol-9-yl)-2-(4-{13-chloro-4-azatricyclo [9.4.0.0^{3,8}]pentadeca-1(15),3(8),4,6,11,13-hexaen-2-ylidene} piperidin-1-yl)ethan-1-one (**4a**)*

4a was synthesized according to general procedure described in Section 4.2.2 by using desloratadine (**8**), carbazole (**9**) and bromoacetyl bromide (**16**). Yield = 78.3%; Rf = 0.49; m.p. 241–243 °C; HPLC purity = 98.19% (C_{18} RP, MeOH:H_2O, 95:5). T_R = 8.339 min. ^{1}H NMR (300 MHz, $CDCl_3$): 8.41 (d, 1H, *J* = 6.9 Hz, Ar-H), 7.73 (d, 1H, *J* = 8.1 Hz, Ar-H), 7.50 (d, 2H, *J* = 7.5 Hz, Ar-H), 7.40 (d, 2H, *J* = 7.2 Hz, Ar-H), 7.06 (m, 8H, Ar-H), 3.21 (s, 2H, CH_2), 3.06–2.94 (m, 4H, CH_2); 2.55–2.32 (m, 4H, CH_2), 2.19–2.12 (m, 4H, CH_2). ^{13}C NMR (75 MHz, $CDCl_3$): 168.4, 157.4, 143.9, 137.5, 136.8 (2C), 134.4, 134.2 (2C), 133.8 (2C), 131.1, 126.0 (2C), 123.5 (2C), 122.3 (2C), 120.7, 119.1 (2C), 117.6 (2C), 114.3, 112.8 (2C), 57.5 (2C), 55.2, 31.8 (2C), 293, 28.5. LC-MS found for $C_{33}H_{28}ClN_3O$ (*m/z*) = 518.2 [M + H +].

Analysis calcd: C, 76.51; H, 5.45; N, 8.11, Found C, 76.47; H, 5.43; N, 8.12.

4.5.2. 2-{1-[6-(9H-carbazol-9-yl)hexyl] piperidin-4-ylidene}-13-chloro-4-azatricyclo[9.4.0.0^{3,8}] pentadeca-1(11),3(8),4,6,12,14-hexaene (**4b**)

4b was synthesized according to general procedure described in Section 4.2.2 by using **8, 9** and 1,6-diiodohexane (**18**). Yield = 74%; R_f = 0.49 (*n*-hexanes/ethyl acetate 9:1); HPLC purity = 98.15% (C_{18} RP, MeOH:H_2O, 95:5). T_R = 6.27 min. m.p. 221–223 °C; ^{1}H NMR (300 MHz, DMSO-d_6): δ 8.71 (d, 1H, J = 6.3 Hz, Ar-H), 7.69 (d, 1H, J = 8.1 Hz, Ar-H), 7.42 (d, 4H, J = 7.8 Hz, Ar-H), 7.20–7.10 (m, 8H, Ar-H), 3.88 (t, 2H, J = 6.9 Hz, CH_2), 299–2.85 (m, 4H, 2 × CH_2), 2.40–2.34 (m, 6H, CH_2), 1.97 (t, 4H J = 10.2 Hz, 2 × CH_2), 1.76–1.67 (m, 2H, 2 × CH_2), 1.44–1.30 (m, 6H, 2 × CH_2); ^{13}C NMR (75 MHz, DMSO-d_6): 157.8, 144.1, 141.2, 137.2, 136.8(2), 136.1, 135.0, 133.1, 132.8(2), 128.0, 127.4, 126.7, 123.4, 115.6, 122.4, 120.3(2), 119.6(2), 118.4(2), 116.9(2), 109.2(2), 62.3, 58.2(2), 55.2, 35.1(2), 33.8, 27.8, 26.7, 26.2. LC-MS found for $C_{37}H_{38}ClN_3$ = 560.2 $[M+H]^+$. Analysis calcd: C, 79.33; H, 6.84; N, 7.50. Found C, 79.39; H, 6.82; N, 7.48.

4.6. Synthesis of heterodimer of 4-(4-methoxyphenyl)-2-thioxo-3,4-tetrahydro-5H-indeno[1,2-d]pyrimidin-5-one and desloratadine (4c)

Synthesis of **4c** was carried out via the synthesis of tricyclic indeno-DHPM (**25**) by following procedure.

A mixture of 1,3-indanedione (**25**, 20 mmol), benzaldehyde (**23**, 20 mmol), Thiourea (**24**, 36 mmol) and $SnCl_2{\cdot}H_2O$ (20 mol %) in ACN were heated to reflux for 5–6 h. Upon completion of reaction, solution was poured to ice with continuous stirring. Precipitates were obtained, filtered and washed with ethanol and recrystallize it with ethanol. ^{1}H NMR (300 MHz, DMSO-d_6): δ 8.71 (brs, 1H, –NH), 7.84 (d, 1H, J = 7.8 Hz, Ar-H), 7.63 (br s, 1H, –NH), 7.43 (m, 1H, Ar-H), 7.41 (m, 1H, Ar-H), 7.28 (t, 1H, J = 7.8 Hz, Ar-H), 7.14 (m, 5H, Ar-H), 5.11 (s, 1H, –CH).

4.6.1. General procedure for the synthesis of heterodimer 25 and desloratadine (4c)

4c was synthesized according to general procedure described in Section 4.2.2 by using **8, 25** and 1,6-diiodohexane (**29**). Yield = 74%; R_f = 0.49 (*n*-hexanes/ethyl acetate 9:1); HPLC purity = 100% (C_{18} RP, MeOH:H_2O, 95:5). T_R = 12.229 min. m.p. 221–223 °C; ^{1}H NMR (300 MHz, DMSO-d_6): δ 8.69 (brs, 1H, –NH), 8.42 (d, 1H, J = 7.2 Hz, Ar-H), 7.48–7.45 (m, 2H, Ar-H), 7.39–7.31 (m, 3H, Ar-H), 7.20–7.09 (m, 9H, Ar-H), 5.12 (s, 1H, –CH), 2.91–2.79 (m, 6H), 2.39–2.28 (t, 6H), 1.74–1.65 (m, 6H), 1.39–1.33 (m, 6H). ^{13}C NMR (75 MHz, DMSO-d_6): 194.1, 162.4, 155.8, 153.2, 148.1, 141.2, 140.6, 137.2, 135.9, 135.1, 134.4, 134.2, 133.4 (2C), 132.7, 129.6, 129.1, 128.9, 128.0, 127.8, 128.1(2), 127.6, 126.7, 125.0, 124.4, 123.5, 113.0, 103.9, 57.2 (2C), 55.1, 53.9, 34.1 (2C), 33.0, 32.4, 29.3, 28.8, 27.6, 25.9, 24.8; LC-MS found for $C_{42}H_{41}ClN_4OS$ = 685.2 [M + H +]. Analysis calcd: C, 73.61; H, 6.03; N, 8.18; S, 4.68. Found C, 73.50; H, 6.06; N, 8.21; S, 4.70.

4.7. In vitro AChE and BChE inhibition studies

In vitro bioassays were performed according to our previously reported procedure [16,26,27]. All the synthesized compounds assayed for their AChE (*Electrophorous electricus* type-VI-S, Sigma-Aldrich GmbH 4USA, code 1001596210) and BChE inhibition (Equine serum Lyophilized Sigma-Aldrich GmbH USA, code 101292670) by our previously reported modified Ellman's method using μQuant microplate spectrophotometer (MQX200, BioTek USA). Stock solution of the synthesized quinazoline was prepared with 0.1 M phosphate buffer (KH_2PO_4/K_2HPO_4) having of pH 8.0. Appropriate amount of DTNB (Ellman's reagent), quinazoline compounds, 0.03 U/ml of enzymes (AChE and BChE) were reacted by pre-incubating at 30 °C for 10 min and then further incubating for 15 min after addition of 1 mM ATCI or BTCI. Each reading was taken in triplicate and the IC_{50} values were obtained by plotting sample concentration verses the inhibition.

4.8. Docking studies

Docking experiments were performed *via* Molecular Operating Environment (MOE) docking program version 2016.08. Downloaded protein and ligand preparation was carried out according to our previous reported procedure [32]. Crystal structure of *Tc*AChE (PDB code: 2CKM, Resolution 2.15 Å) in complex with alkylene-linked *bis*-tacrine (7 carbon linker) as native ligand was selected for these studies. All the water molecules were removed from the protein structure, then hydrogen atoms were added and energy optimization was carried out using default force field. The three-dimensional (3D) structures of compounds were modelled through the builder program implemented in MOE. The geometrical parameters for 3D structures of the compounds were optimized, and partial charges were calculated before docking. The 3D protonation of the 2CKM was done and energy minimization of the retrieved protein molecule was carried out by using default parameters of MOE energy minimization algorithm [gradient: 0.05, Force Field: MMFF94X]. The resulting model was subjected to systematic conformational search at default parameters with RMS gradient of 0.01 kcal/mol using Site Finder. The active site of the enzyme was defined within 10 Å of the native ligand B7T. The lowest energy minimized pose was used for further analysis. Ligand-interaction module of MOE was used to calculate the 2D ligand-enzyme interactions. The view of the docking results and analysis of their surface with graphical representations were done using MOE and discovery studio visualizer [33].

Acknowledgement

Dr. Umer Rashid is thankful to Higher Education Commission Pakistan for financial support under HEC-NRPU project 5291/Federal/NRPU/R&D/HEC/2016. MOE 2016.08 license is funded under this project.

Appendix A. Supplementary material

Supplementary data to this article can be found online at https://doi.org/10.1016/j.bioorg.2018.10.035.

References

[1] U. Rashid, F.L. Ansari, Challenges in designing therapeutic agents treating Alzheimer 's disease-form serendipity to rationality, in: Drug Design Discovery in Alzheimer 's Disease, Elsevier, 2014, pp. 40–141.
[2] H. Soreq, S. Seidman, Acetylcholinesterase–new roles for an old actor, Nat. Rev. Neurosci. (2001) 294–302.
[3] T.H. Ferreira-Vieira, I.M. Guimaraes, F.R. Silva, F.M. Ribeiro, Alzheimer's disease: targeting the cholinergic system, Curr. Neuropharmacol. 14 (1) (2016) 101–115.
[4] M. Harel, J.L. Sussman, E. Krejci, S. Bon, P. Chanal, J. Massoulié, I. Silman, Conversion of acetylcholinesterase to butyrylcholinesterase: modeling and mutagenesis, Proc. Nat. Acad. Sci. 89 (22) (1992) 10827–10831.
[5] D. Galimberti, E. Scarpini, Old and new acetylcholinesterase inhibitors for Alzheimer's disease, Expert. Opin. Investig. Drugs 25 (10) (2016) 1181–1187.
[6] L. Savini, A. Gaeta, C. Fattorusso, B. Catalanotti, G. Campiani, L. Chiasserini, C. Pellerano, E. Novellino, D. McKissic, A. Saxena, Specific targeting of acetylcholinesterase and butyrylcholinesterase recognition sites. Rational design of novel, selective, and highly potent cholinesterase inhibitors, J. Med. Chem 46 (1) (2003) 1–4.
[7] F. Mangialasche, A. Solomon, B. Winblad, P. Mecocci, M. Kivipelto, Alzheimer's disease: clinical trials and drug development, Lancet Neurol. 9 (7) (2010) 702–716.
[8] M. Singh, M. Kaur, H. Kukreja, R. Chugh, O. Silakari, D. Singh, Acetylcholinesterase inhibitors as Alzheimer therapy: from nerve toxins to neuroprotection, Eur. J. Med. Chem 70 (2013) 165–188.
[9] H. Sugino, A. Watanabe, N. Amada, M. Yamamoto, Y. Ohgi, D. Kostic, R. Sanchez, Global trends in Alzheimer disease clinical development: increasing the probability of success, J. Clin. Therap. 37 (8) (2015) 1632–1642.
[10] G. Johnson, S.W. Moore, The peripheral anionic site of acetylcholinesterase: structure, functions and potential role in rational drug design, Curr. Pharm. Des. 12

(2) (2006) 217–225.
[11] Y. Bourne, P. Taylor, Z. Radić, P. Marchot, Structural insights into ligand interactions at the acetylcholinesterase peripheral anionic site, EMBO J. 22 (1) (2003) 1–12.
[12] L.M. Eubanks, C.J. Rogers, A.E. Beuscher, G.F. Koob, A.J. Olson, T.J. Dickerson, K.D. Janda, A molecular link between the active component of marijuana and Alzheimer's disease pathology, Mol. Pharm 3 (6) (2006) 773–777.
[13] A. Castro, A. Martinez, Peripheral and dual binding site acetylcholinesterase inhibitors: implications in treatment of Alzheimer's disease, Mini. Rev. Med. Chem. 1 (2001) 267–272.
[14] M.L. Bolognesi, V. Andrisano, M. Bartolini, R. Banzi, C. Melchiorre, Propidium-based polyamine ligands as potent inhibitors of acetylcholinesterase and acetylcholinesterase-induced amyloid-β aggregation, J. Med. Chem 48 (1) (2005) 24–27.
[15] L. Peauger, R. Azzouz, V. Gembus, M.L. Ţînţaş, J. Sopková-de Oliveira Santos, P. Bohn, C. Papamicaël, V. Levacher, Donepezil-based central acetylcholinesterase inhibitors by means of a bio-oxidizable prodrug strategy: design, synthesis, and in vitro biological evaluation, J. Med. Chem 60 (13) (2017) 5909–5926.
[16] S. Ahmad, F. Iftikhar, F. Ullah, A. Sadiq, U. Rashid, Rational design and synthesis of dihydropyrimidine based dual binding site acetylcholinesterase inhibitors, Bioorg. Chem 69 (2016) 91–101.
[17] M.L. Bolognesi, A. Cavalli, L. Valgimigli, M. Bartolini, M. Rosini, V. Andrisano, M. Recanatini, C. Melchiorre, Multi-target-directed drug design strategy: from a dual binding site acetylcholinesterase inhibitor to a trifunctional compound against Alzheimer's disease, J. Med. Chem 50 (26) (2007) 6446–6449.
[18] P. Muñoz-Ruiz, L. Rubio, E. García-Palomero, I. Dorronsoro, M. del Monte-Millán, R. Valenzuela, P. Usán, C. de Austria, M. Bartolini, V. Andrisano, A. Bidon-Chanal, M. Orozco, F.J. Luque, M. Medina, A. Martínez, Design, synthesis, and biological evaluation of dual binding site acetylcholinesterase inhibitors: new disease-modifying agents for Alzheimer's disease, J. Med. Chem 48 (23) (2005) 7223–7233.
[19] Y.F. Han, C.P. Li, E. Chow, H. Wang, Y.P. Pang, P.R. Carlier, Dual-site binding of bivalent 4-aminopyridine- and 4-aminoquinoline-based AChE inhibitors: contribution of the hydrophobic alkylene tether to monomer and dimer affinities, Bioorg. Med. Chem 7 (1999) 2569–2575.
[20] L. Savini, G. Campiani, A. Gaeta, C. Pellerano, C. Fattorusso, L. Chiasserini, J.M. Fedorko, A. Saxena, Novel and potent tacrine-related hetero- and homobivalent ligands for acetylcholinesterase and butyrylcholinesterase, Bioorg. Med. Chem. Lett 11 (2001) 1779–1782.
[21] P.R. Carlier, Y.F. Han, E.S. Chow, C.P. Li, H. Wang, T.X. Lieu, H.S. Wong, Y.P. Pang, Evaluation of short-tether bis-THA AChE inhibitors. A further test of the dual binding site hypothesis, Bioorg. Med. Chem 7 (1999) 351–357.
[22] C. Guillou, A. Mary, D.Z. Renko, E. Gras, C. Thal, Potent acetylcholinesterase inhibitors: design, synthesis and structureactivity relationships of alkylene linked bis-galanthamine and galanthamine-galanthaminium salts, Bioorg. Med. Chem. Lett 10 (2000) 637–639.
[23] D. Torrero, M. Scarpellini, E. Viayna, A. Badia, M.V. Clos, A. Camins, M. Pallàs, M. Bartolini, F. Mancini, V. Andrisano, J. Estelrich, M. Lizondo, A. Bidon-Chanal, F.J. Luque, Novel donepezil-based inhibitors of acetyl- and butylcholinesterase and acetylcholinesteraseinduced β-amyloid aggregation, J. Med. Chem. 51 (2008) 3588–3598.
[24] B. Tasso, M. Catto, O. Nicolotti, F. Novelli, M. Tonelli, I. Giangreco, L. Pisani, A. Sparatore, V. Boido, A. Carotti, Quinolizidinyl derivatives of bi-and tricyclic systems as potent inhibitors of acetyl-and butyrylcholinesterase with potential in Alzheimer's disease, Eur. J. Med. Chem 46 (2011) 2170–2184.
[25] G. Tin, T. Mohamed, N. Gondora, M.A. Beazelya, P.P. Rao, Tricyclic phenothiazine and phenoselenazine derivatives as potential multi-targeting agents to treat Alzheimer's disease, Med. Chem. Commun 6 (2015) 1930–1941.
[26] N. Sultana, M. Sarfraz, S.T. Tanoli, M.S. Akram, A. Sadiq, U. Rashid, M.I. Tari, Synthesis, Crystal structure determination, biological screening and docking studies of N1-substituted derivatives of 2,3-dihydroquinazolin-4(1H)-one as inhibitors of cholinesterases, Bioorg. Chem 72 (2017) 256–267.
[27] M. Sarfraz, N. Sultana, U. Rashid, M.S. Akram, A. Sadiq, M.I. Tariq, Synthesis, biological evaluation and docking studies of 2,3-dihydroquinazolin-4(1H)-one derivatives as inhibitors of cholinesterases, Bioorg. Chem 70 (2017) 237–244.
[28] G.Z. Liu, H.W. Xu, G.W. Chen, P. Wang, Y.N. Wang, H.M. Liu, D.Q. Yu, Stereoselective synthesis of desloratadine derivatives as antagonist of histamine, Bioorg. Med. Chem 18 (2010) 1626–1632.
[29] S. Mu, Y. Liu, M. Gong, D.K. Liu, C.X. Liu, Synthesis and biological evaluation of substituted desloratadines as potent arginine vasopressin V2 receptor antagonists, Molecules 19 (2014) 2694–2706.
[30] H.M. Gijsen, D. Berthelot, M.A. De Cleyn, I. Geuens, B. Brône, M. Mercken, Tricyclic 3,4-dihydropyrimidine-2-thione derivatives as potent TRPA1 antagonists, Bioorg. Med. Chem. Lett 22 (2012) 797–800.
[31] Molecular Operating Environment (MOE), 2016.08; Chemical Computing Group ULC, 1010 Sherbooke St. West, Suite #910, Montreal, QC, Canada, H3A 2R7, 2018.
[32] F. Iftikhar, F. Yaqoob, N. Tabassum, M.S. Jan, A. Sadiq, S. Tahir, T. Batool, B. Niaz, F.L. Ansari, M.I. Chaudhary, U. Rashid, Design, Synthesis, In-Vitro Thymidine Phosphorylase Inhibition, In-Vivo Antiangiogenic and In-Silico Studies of C-6 substituted dihydropyrimidines, Bioorg. Chem. 80 (2018) 99–111.
[33] Dassault Systèmes BIOVIA, Discovery Studio Modelling Environment, Release 4.5, San Diego: Dassault Systems, 2015.